 MCB, vol.4, no.1, pp.1-12, 2007

Orientation of Apical and Basal Actin Stress Fibers in Isolated and Subconfluent Endothelial Cells as an Early Response to Cyclic Stretching

Hiroshi Yamada[*†] **and Hirokazu Ando**[†]

Abstract: We investigated the response of apical and basal actin stress fibers (SFs) and its dependency on cell confluency for endothelial cells subjected to cyclic stretching. Porcine aortic endothelial cells from the 2^{nd} and 5^{th} passages were transferred to a fibronectin-coated silicone chamber with 5000–8000 cells/cm^2 (isolated condition), positioning the cells apart, or with 25,000–27,000 cells/cm^2 (subconfluent condition), allowing cell-to-cell contact. The substrate was stretched cyclically by 0.5 Hz for 2 h with a peak strain on the substrate that was 15% in the stretch direction and –4% in the transverse direction. The actin filaments (AFs) were stained with rhodamine phalloidin and their orientations were examined under a confocal laser scanning microscope. In the basal region, SFs formed in all of the cells under both the isolated and subconfluent conditions. We observed an average of 5 and 9 SFs per cell under the isolated and subconfluent conditions, respectively, in the fluorescent images of the apical region. We also observed cells that were bush-like without apical AFs or apical SFs. On average, the SFs in the subconfluent cells oriented in the direction of minimal strain, while the SFs in the isolated cells oriented in the direction of a 2% compressive strain. These results suggest that such differential response may be due to differences in the transmission of mechanical stretching to the central and apical regions of the cell through the SFs. We also speculate that cell-to-cell contact might change the strength, orientation, and anchorage of apical AFs and play a critical role in mechanical signal transduction.

[*] Corresponding author. Phone: +81 93 695 6031; Fax: +81 93 695 6005; E-mail: yamada@life.kyutech.ac.jp

[†] Department of Biological Functions and Engineering, Graduate School of Life Science and Systems Engineering, Kyushu Institute of Technology. 2-4 Hibikino, Wakamatsu-Ku, Kitakyushu 808-0196, Japan.

Keyword: stress fiber, orientation, cyclic stretching, endothelial cell, deformation

1 Introduction

Vascular endothelial cells are exposed to cyclic stretching and fluid shear stress and orient along the vascular axis *in vivo* (Flaherty *et al*., 1972; Langille and Adamson, 1981; Sipkema *et al*., 2003). Under cyclic stretching, actin SFs in the basal region of the cell remodel to orient within a limited angle range at the subcellular level (Dartsch and Betz, 1989; Takemasa *et al*., 1997, 1998; Yoshigi *et al*., 2003). This response is thought to be the result of adaptation to or survival from such mechanical environments (Takemasa *et al*., 1998). It has been suggested in the literature that remodeling of actin cytoskeleton and cell reorientation are the minimization of mechanical strains to actin filaments and cells, respectively (Wang *et al*., 1995; Takemasa *et al*., 1997, 1998). The detailed response of SFs to such mechanical stimuli, specifically the orientation angle and location of SFs, is not fully understood. The morphological response of SFs to cyclic stretching is usually described in terms of angles (peak, variation, and range). The distribution of AFs/SFs has been delineated quantitatively as a function of mechanical strain (Takemasa *et al*., 1998; Yamada *et al*., 2000, 2002) or stress (Ingber, 1997; Stamenovic and Ingber, 2002).

The limited orientation range of SFs is predicted from the hypothesis that each SF exists if its strain does not exceed a certain threshold, *e.g.*, 5% (Yamada *et al*., 2002). Previous experimental results (Dartsch and Betz, 1989; Takemasa *et al*., 1998; Yoshigi *et al*., 2003) demonstrated that this hypothesis holds for SFs in the basal region of the cell (Yamada *et al*., 2002). However, there is ev-

idence that SFs or AFs exist in the apical region (White and Fujiwara, 1986; Kano *et al*., 2000) or in the area between the apical and basal membranes of the cell (Wang *et al*., 2000a). Wang *et al*. (2000a) reported that after 1 h of cyclic equibiaxial stretching with a 10% strain range, the actin cytoskeleton was remodeled into a three-dimensional, "tent-like" actin structure. In their fluorescent image, there are no SFs along the basal membrane of the cell. This result supports the hypothesis that predicts the out-of-plane orientation of SFs (Yamada *et al*., 2006). Simultaneously, this raises the question, can one observe SFs in regions other than the cell bottom in a cell subjected to cyclic uniaxial stretching *in vitro*, which is the same type of deformation *in vivo*?

Numerical simulations of the three-dimensional orientation angles of SFs suggest that SFs are located in the apical region of the cell under cycles of pure uniaxial stretching (stretching in one direction with a deformation constraint in the transverse direction) (Yamada *et al*., 2002). Fujiwara and coworkers reported one piece of experimental evidence, the existence of SFs at the apical membrane of aortic endothelial cells *in situ* in the rat and guinea pig (White and Fujiwara, 1986; Kano *et al*., 2000). In their studies, the cells in the aorta were subjected to the blood flow in normotensive or spontaneously hypertensive conditions. Their findings support the theoretical prediction of SF location.

The purpose of this study was to evaluate and compare the early responses of the reorientation of apical and basal SFs to cyclic uniaxial stretching under the conditions of isolated and subconfluent cell densities. We imposed cyclic uniaxial stretching, which is similar to *in vivo* stretching, on cultured porcine aortic endothelial cells. We examined the existence and orientation angle of SFs/AFs in the apical and basal regions of isolated and subconfluent cells under confocal laser scanning microscopy. By choosing the two locations, *i.e.*, apical and basal regions, and two populations of cells, *i.e.*, isolated and subconfluent cells, we investigated the effects of the location in the cell and cell-to-cell contact on the orientation of SFs/AFs.

2 Methods

2.1 Materials and cell culture

Porcine thoracic aortas were obtained from a slaughterhouse. The excised aortas were opened longitudinally and the lumen was gently stroked with a surgical blade. The removed endothelial cells were dispersed in 35-mm dishes coated with Type I collagen (Iwaki, Japan), which were filled with Dulbecco's modified Eagle's medium (Gibco, USA) containing 10% fetal bovine serum (Gibco) and a 1% mixture of penicillin, streptomycin, and neomycin (Gibco). The cells were cultured at 37°C in an incubator in a 100% humidified atmosphere containing 5% carbon dioxide. When the cells became 70–80% confluent after seeding, they were subcultured repeatedly in 35-mm tissue culture dishes (Iwaki) using 0.05% trypsin–EDTA (Gibco).

A silicone chamber with a 32 × 32-mm bottom membrane (10-cc type; Strex, Japan) was coated with 1 ml of 50 μg/ml fibronectin from porcine plasma (Wako Pure Chemical Industries, Japan). Cells from the 2^{nd} to 5^{th} passages were transferred to the silicone membrane at a density of 5000 to 8000 cells/cm^2 (isolated condition) to avoid cell-to-cell contact and 25,000–27,000 cells/cm^2 (subconfluent condition) to allow contact between adjacent cells. The term "cell-to-cell contact" is used for a cell in which some part of the border contacts another cell. After incubation overnight (12–16 h), phase-contrast images were acquired to confirm the cell density. Then, the chamber was mounted on the stretching apparatus.

2.2 Repeated stretching and acquisition of SF images

To investigate the orientation of actin SFs, the silicone membrane was subjected to 15% uniaxial stretching associated with 4% transverse compression with a 0.5-Hz triangular waveform for 2 h, using a pair of pulse stages and a programmable controller (PS-30E-0 & CAT II; Chuo Precision Industrial, Japan). The temperature of the cells was kept constant by soaking the chamber in a bath kept at 37°C with a thermoplate (MATS-55R30T; Tokai Hit, Japan). Before the stretch-

ing test, the region of interest in the silicone substrate, *i.e.*, the central 10 × 10-mm square, was examined to ensure that it deformed as expected by tracing five sets of four fine ink marks, which were located at the center and four corners of the region of interest and were plotted at 1-mm intervals on the membrane. For all measured locations in the four silicone chambers, the strains (mean ± SD) in the stretch and transverse directions varied as 15.45 ± 0.18% and–4.20 ± 0.12%, respectively.

After stretching, the cells were fixed in 4% paraformaldehyde for 5 min. Then, the cells were permeabilized in 0.25% Triton X-100 (Alfa Aesar, USA) in phosphate-buffered saline (Gibco) for 5 min. Finally, the cells were stained with 0.165 μM rhodamine phalloidin (Molecular Probes, USA) for 20 min.

Images of 600 × 800 pixels were acquired for cells in the central 10 × 10-mm square with a resolution of $\times$0.167gpixel/μm. The cells were scanned at a slice interval of 0.25 μm over a range of 10 μm in height under confocal laser scanning microscopy (FV300-BX51WI; Olympus, Japan) with 60$\times$ water immersion objective. Regions of interest for image acquisition were chosen randomly; under the isolated condition they only covered a single cell, and under the subconfluent condition they covered at least a single cell with some parts of the contacting surrounding cells. Cell-to-cell contact was confirmed from a fluorescent image showing that the boundary of the cell of interest overlapped onto or shared a boundary with the neighbors.

2.3 Data analysis

We chose the basal SF image that had the greatest fluorescence intensity and the apical SF/AF image that had the clearest structure of SFs/AFs in the upper portion of the cell. In each image, a stained line segment in the apical and basal regions was identified as a SF and a woven segment in the apical region was identified as an AF. The orientation angles of SFs in the apical and basal regions, which we termed apical and basal SFs, respectively, were obtained by measuring the angle between a superposed straight line on a SF and the direction of stretch in the fluorescent image. The SFs in the dense peripheral band of the cell were not counted. In the basal region, the major axis of the cell, or the cell axis, was found by fitting an ellipse to the cell outline. To measure the SF angles with respect to a reference axis, the positive direction of the stretching axis was defined so that the cell axis was <90^{o} (see Fig. 1). The range of SF angles was defined to fall between 0 and 180^{o}.

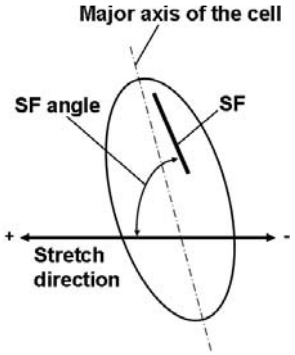

Figure 1: Definition of the orientation angle of a SF as measured with respect to the positive axis of the stretch direction.

2.4 Statistical analysis

For the orientations of SF/cell groups, Wilcoxon's matched-pairs signed-ranks test or the Mann–Whitney U-test was used to compare the medians of the differences between the pairs of two groups or the medians of two groups, respectively. Two distributions were considered to be significantly different if p<0.01. StatView version 5 (SAS Institute, USA) was used for the statistical computations.

2.5 Estimation of a basal SF angle based on the substrate deformation

The strain of a SF was calculated by comparing its length on the maximally stretched substrate with that on the unstretched substrate using the kinematic relation for the silicone substrate under uniaxial stretching (Yamada *et al*., 2002). The SF strain is a function of its angle in the unstretched state and a function of the deformation of the SFs in the cell (Yamada *et al*., 2006).

Denoting the angle of a basal SF (a line segment with a unit length) in the unstretched state as θ, and the stretch (deformed length/undeformed length) in the stretch (x-axis) and transverse (y-axis) directions as λ_x and λ_y, respectively, the stretch of the SF (λ_{SF}) can be expressed as

$$\lambda_{SF} = \sqrt{\lambda_x^2 \cos^2\theta + \lambda_y^2 \sin^2\theta}. \quad (1)$$

From this equation, the angle of the SF that has a stretch of λ_{SF} is

$$\theta = \cos^{-1}\sqrt{\frac{\lambda_{SF}^2 - \lambda_y^2}{\lambda_x^2 - \lambda_y^2}}. \quad (2)$$

From experimental measurements of the silicone membranes in the silicone chamber, the deformation of the substrate can be approximated as (Yamada *et al*., 2002)

$$\lambda_x = \lambda, \quad \lambda_y = \lambda^{-0.29}. \quad (3)$$

For example, if the strain of basal SFs is limited to $0.99 \leq \lambda_{SF} \leq 1.01$, the corresponding angle range for $0 \leq \theta \leq \pi/2$ will be

$$\cos^{-1}\sqrt{\frac{1.01^2 - \lambda^{-0.58}}{\lambda^2 - \lambda^{-0.58}}} \leq \theta \leq \cos^{-1}\sqrt{\frac{0.99^2 - \lambda^{-0.58}}{\lambda^2 - \lambda^{-0.58}}}. \quad (4)$$

3 Results

Table 1 summarizes the numbers of cells used for the data analysis and SFs counted in the apical and basal regions of isolated and subconfluent cells. Cells were selected from five experiments under the isolated condition, and from two experiments under the subconfluent condition. Cells were categorized into two groups: cells with both apical and basal SFs and those with basal SFs, but no apical SFs. The former group had roughly one-tenth as many apical SFs as basal SFs. The height of the chosen image slice for apical SF measurements was 3.7 ± 0.7 μm (mean $\pm$ SD) for isolated cells and 3.0 ± 0.4 μm for subconfluent cells with respect to the basal SF image slice. In the latter group, apical AFs were observed for all of the subconfluent cells, but not for isolated cells.

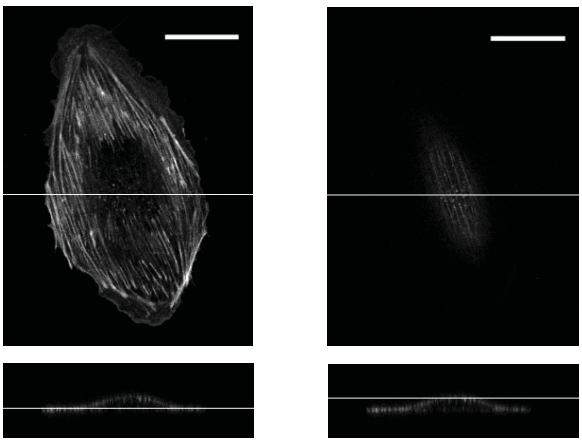

(a) (b)

Figure 2: Typical example of the distribution of SFs/AFs in the (a) basal (reference height: 0 μm) and (b) apical regions (height: 3.25 μm) of isolated cells that have apical SFs (Bar: 20 μm). Horizontal (top panel) and vertical (bottom panel) cross sections of each region are shown. The stretching axis is in the horizontal direction.

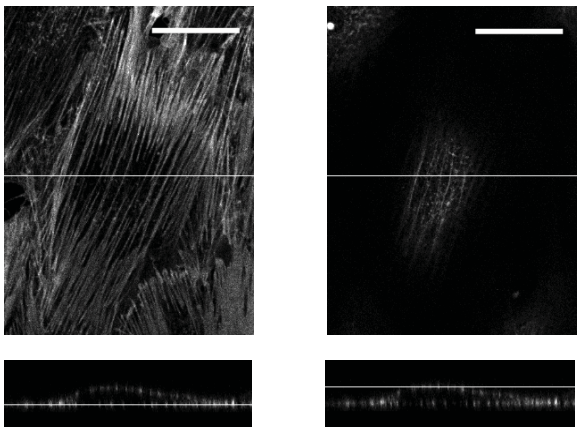

(a) (b)

Figure 3: Typical example of the distribution of SFs/AFs in the (a) basal (reference height: 0 μm) and (b) apical regions (height: 3.5 μm) of subconfluent cells that have apical SFs (Bar: 20 μm).

For the group of cells that had both apical and basal SFs, typical examples of the distribution of SFs/AFs in the basal and apical regions are shown in Figs. 2 and 3 for isolated and subconfluent

Table 1: Numbers of cells used for the data analysis and SFs counted in the apical and basal regions.

Cell density	Location of SFs	Number of cells	Number of SFs	
			Apical	Basal
Isolated	Both apical and basal	25	131	1308
	Basal only	19	none	829
Subconfluent	Both apical and basal	11	103	607
	Basal only	20	none	1088

cells, respectively. In an isolated cell, each bundle of basal SFs was thin, short, and oriented over a certain range. In the basal region, one end of the SF was usually at or near the cell margin and the other was near the center of the cell; in contrast, in the apical region, there were straight line-like SF structures and bush-like AF structures. In the subconfluent cells, there was an orderly structure of SF bundles in the basal region. Each bundle of basal SFs was thick, long, and oriented over a narrower range, ending primarily at the margin of the cell at both ends, while in the apical region, SF and AF structures developed in a small area, reflecting the basal SF development.

Figure 4 shows the cell axis and orientation (mean $\pm$ SD) of the apical and basal SFs in individual cells for the group of cells that had both apical and basal SFs, and the correlation of the mean angles between apical and basal SFs in individual cells. The correlation coefficient was 0.48 and 0.51 in isolated and subconfluent cells, respectively, and the mean angles were uncorrelated (p>0.01) between apical and basal SFs in both cell groups. Wilcoxon's tests showed no statistically significant differences among the median angles of the apical and basal SFs and the angle of the individual cells. Wilcoxon's tests for the median range of SF angles in individual cells also indicated that individual cells under the isolated condition had a wider angle range in basal SFs versus apical SFs; a wider angle range was also observed in basal SFs when no apical SFs were present versus when apical SFs were present, and in basal SFs under the isolated condition versus the subconfluent condition (see Table 2).

The orientation of each SF was summed over all the cells to determine the distribution pattern for the cell population. Histograms of the orientation of apical and basal SFs are shown in Fig. 5 for isolated cells and in Fig. 6 for subconfluent cells, comparing cells that had both apical and basal SFs and those that had basal SFs, but no apical SFs. The angles (mean $\pm$ SD) of the apical SFs, basal SFs, and cell axis are listed in Table 3. Using the Mann-Whitney U-test, statistically significant differences (p <0.01) were detected in the median SF angles among the SF groups in Table 3, except between apical and basal SFs in the isolated cells and between basal SFs in the subconfluent cells that had both apical and basal SFs and those that only had basal SFs.

Figure 7 shows the predicted angles of SFs in the unstretched configuration. The SFs were subjected to strains of –0.05, –0.01, 0, 0.01, or 0.05 under the deformation of the substrate defined by a stretch of λ = 1.0-1.3 in the stretch direction and an associated stretch of $\lambda^{-0.29}$ in the transverse direction. Figure 7 compares these calculated results with the distribution of the orientation angle of basal SFs for isolated and subconfluent cells. The average angle (mean $\pm$ SD) of the SFs was 78.1 $\pm$ 13.2^{o} for isolated cells and 70.2 $\pm$ 10.1^{o} for subconfluent cells. The peak angle of the SF distribution for subconfluent cells (*i.e.*, 60-65^{o}) coincided with 0% strain on the SFs and the peak angle for isolated cells (*i.e.*, 70-75^{o}) corresponded to 2% compressive strain, when the substrate was stretched by 15%. Most of the SFs oriented in the region in which the range of SF strain was <5%.

4 Discussion

Comparing the fluorescent images of basal SFs in isolated (Fig. 2) and subconfluent (Fig. 3) cells, the subconfluent cell has a more orderly, denser structure than the isolated cell. This orderly structure is consistent with the reports for confluent

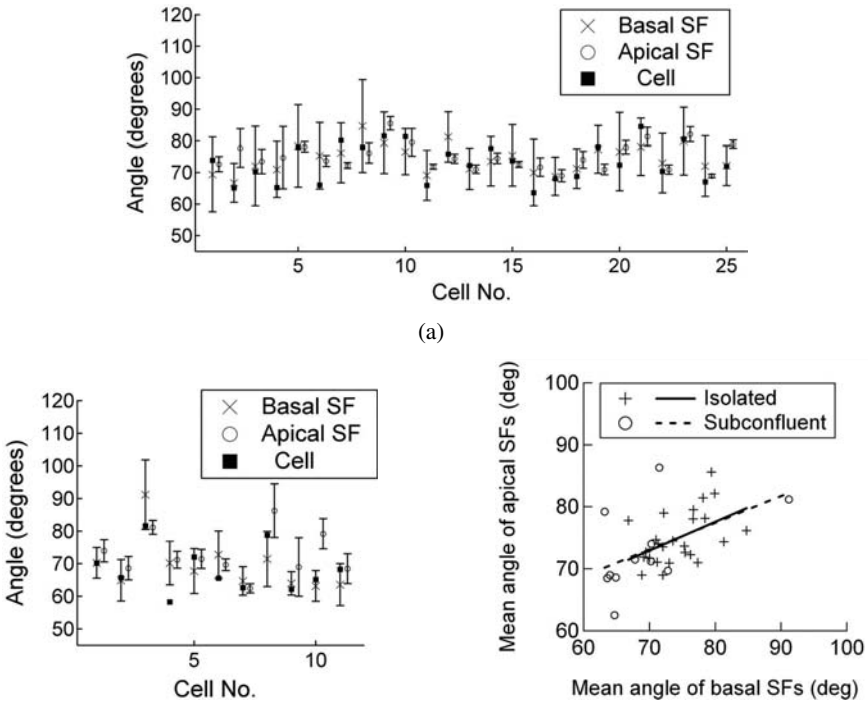

Figure 4: Orientation angle (mean ± SD) of SFs in the basal and apical regions and the major axis in each cell for (a) 25 isolated cells and (b) 11 subconfluent cells both of which have apical SFs, and (c) correlation of the mean angles between apical and basal SFs in individual cells.

Table 2: Standard deviation range (mean ± SD) of the SF angles in individual cells.

Cell density	Location of SFs	SD range of individual cell SF angles	
		Apical	Basal
Isolated	Both apical and basal	$2.5 \pm 2.0^{o*ia}$	$9.3 \pm 2.4^{o*ib}$
	Basal only	–	$13.4 \pm 3.1^{o*io}$
Subconfluent	Both apical and basal	$4.0 \pm 2.5^{o*sa}$	$6.4 \pm 2.0^{o*sb}$
	Basal only	–	$7.4 \pm 2.0^{o*so}$

Statistically significant ($p < 0.01$): *ia *vs* *ib, *ib *vs* *io, ib* *vs* *sb, *io *vs* *so. Not statistically significant: *ia *vs* *sa, *sa *vs* *sb, *sb *vs* *so.

Table 3: Angles (mean ± SD) of cells and the apical and basal SFs.

Cell density	Location of SFs	Angle of cells	Angle of SFs	
			Apical	Basal
Isolated	Both apical and basal	73 ± 6^{o}	$74.8 \pm 5.1^{o*ia}$	$74.2 \pm 10.6^{o*ib}$
	Basal only	85 ± 4^{o}	–	$86.8 \pm 15.3^{o*io}$
Subconfluent	Both apical and basal	68 ± 7^{o}	$73.0 \pm 7.8^{o*sa}$	$70.5 \pm 10.9^{o*sb}$
	Basal only	71 ± 8^{o}	–	$70.2 \pm 10.0^{o*so}$

Statistically significant ($p < 0.01$): *ia *vs* *sa, *ib *vs* *io, ib* *vs* *sb, *io *vs* *so, *sa *vs* *sb. Not statistically significant: *ia *vs* *ib, *sb *vs* *so.

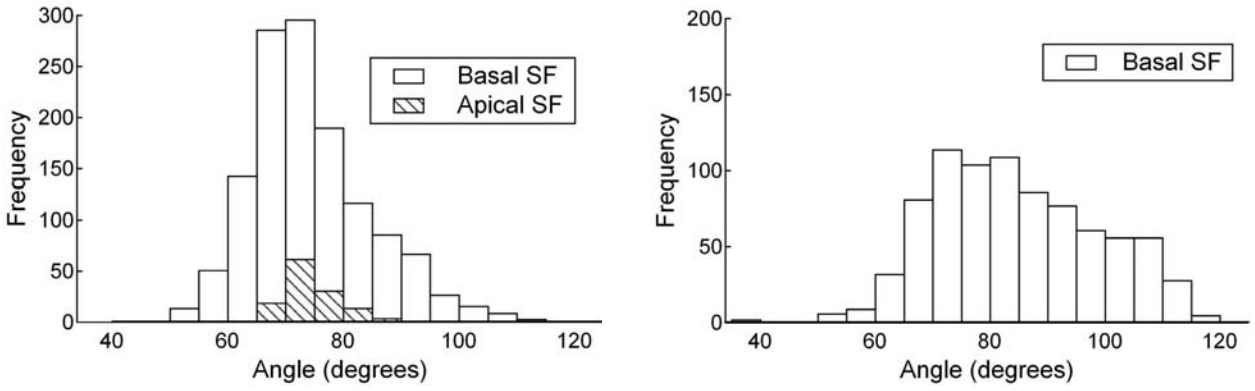

(a) (b)

Figure 5: Orientation distributions of SFs in the basal region for isolated cells that have (a) both apical and basal SFs and (b) basal SFs only.

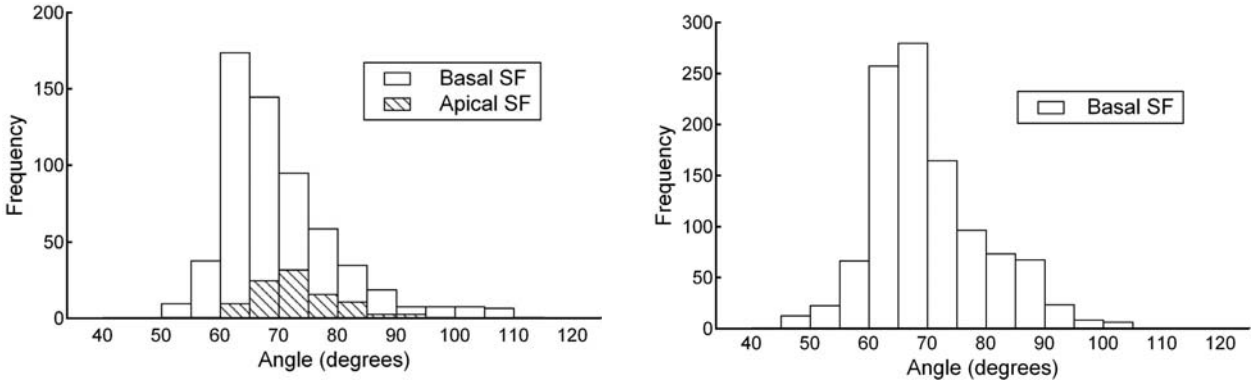

(a) (b)

Figure 6: Orientation distributions of SFs in the basal region for subconfluent cells that have (a) both apical and basal SFs and (b) basal SFs only.

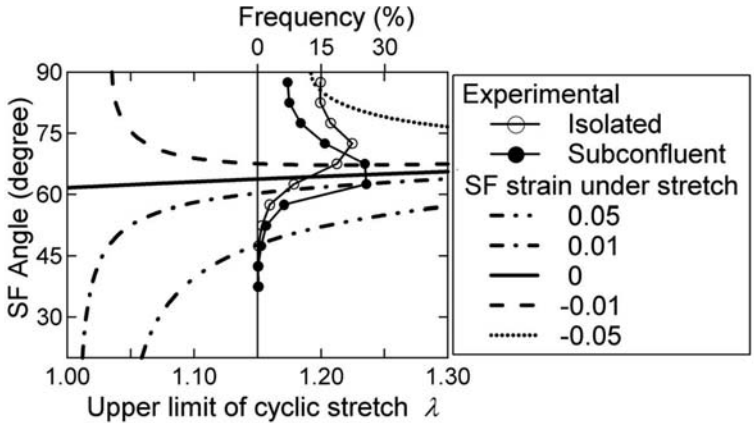

Figure 7: Orientation distributions of SFs in the basal region of isolated and subconfluent cells and a comparison with the predicted angles of SFs with strains of -0.05, -0.01, 0, 0.01, and 0.05 when the substrate is subjected to a strain of λ - 1 in the stretch direction and -0.04 in the transverse direction.

cells by Iba and Sumpio (1991) under 1-Hz cyclic stretching with a 24% strain range for 24 h and by Takemasa *et al*. (1998) under 1-Hz cyclic stretching with a 50% strain range for 30 min. In contrast, before cyclic stretching, the orientations of SFs in cultured human endothelial cells (passages 9–21) without cell-to-cell contact vary; therefore, there is no preferred direction (Wille *et al*., 2004). Wang *et al*. (2000b) investigated the effect of the duration of 10% cyclic pure uniaxial stretching at 0.5 Hz for 0.5, 1, and 3 h on human endothelial cells (passages 5–16), and showed that the median orientation angles of subconfluent cells, defined as between 0 and 90°, were about 50, 78, and 80° after 0, 1, and 3 h, respectively, indicating that the reorientation of subconfluent cells in our study was almost saturated after rapid remodeling.

The difference in the organization of isolated and subconfluent cells is attributable to the transmission of mechanical stretching to the cells as well as the regulation of organizing intracellular SFs/AFs, both of which may be affected by cell-to-cell contact. For cells exposed to a fluid shear stress of 2 Pa for 24 h, Kataoka *et al*. (1998) reported that isolated cells were oriented randomly, whereas the cells in the center of a colony oriented in the flow direction. For both mechanical stimuli, *i.e.*, cyclic stretching and fluid shear stress, linking proteins play an important role by connecting adjacent cells physically and chemically. The cell-to-cell contact was reported to mediate the molecular organization of cell-to-cell junctions as a function of cell confluency (Dejana *et al*., 1995; Lampugnani *et al*., 1995). It also affects the SF reorganization. Wang *et al*. (2001) also speculated that the cell population density was one explanation for the difference in the orientation angle between confluent cells (Dartsch and Betz, 1989) and subconfluent cells (Wang *et al*., 2001) subjected to cyclic stretching.

Physical contact between adjacent cells may transmit the strain of the substrate to a greater height in the cell, which enhances the remodeling of AFs. To investigate the physical effect of cell-to-cell contact, we used a finite element model of a single cell adhering to the substrate, which was created by Yamada and Matsumura ;2004) (See Fig. 8(a)). Briefly, the cell was 6 μm in height, 60 μm in diameter at the cellular bottom, and 1 μm in thickness in the peripheral region. The cell model consisted of cytoplasm and the nucleus, whose shape was an ellipsoid with a 5-μm short axis in the height direction and a 8-μm long axis in the horizontal directions. The cytoplasm, nucleus, and substrate were assumed to be neo-Hookean material, which is incompressible, isotropic, and hyperelastic, and their material constants, which were equal to one-sixth of Young's modulus, were determined to be 129 Pa, 850 Pa, and 129 kPa, respectively. We applied a 15% tensile strain and 4% compressive strain to the substrate to match the experimental conditions. The finite element analysis was performed by Abaqus/standard version 6.6 (Abaqus, USA).

Figure 8(b) shows the distribution of the strain component in the stretch direction of the cell under the above deformation. Note that the substrate was removed from the figure. The peripheral region of the cell had about 15% strain, which was the same as the strain of the substrate. This suggests that the physical cell-to-cell contact in the peripheral region without SF structures will not enlarge the cellular strain. In the central region, which contained a nucleus bulge, a portion had a strain that was less than the applied strain (<0.15) even near the cell bottom. This indicates that the physical cell-to-cell contact in the peripheral region can transmit the strain to an adjacent cell and enlarge the strain in its central region if SFs connect the cell–cell junctions to the central region of the cell. If one end of the SFs is located at a higher level of the cell, the strain in the apical region of the cell will become larger, which might cause the difference between the SF orientations of isolated and confluent cells.

The complete transmission of the strain from the substrate through the extracellular matrix to the basal membrane in isolated cells (Yamada and Mouri, 2006) should also hold for subconfluent cells. The SFs in the subconfluent cells were aligned in the strain-free angle, which was consistent with the result for SFs in confluent cells (Takemasa *et al*., 1997, 1998). The alignment of

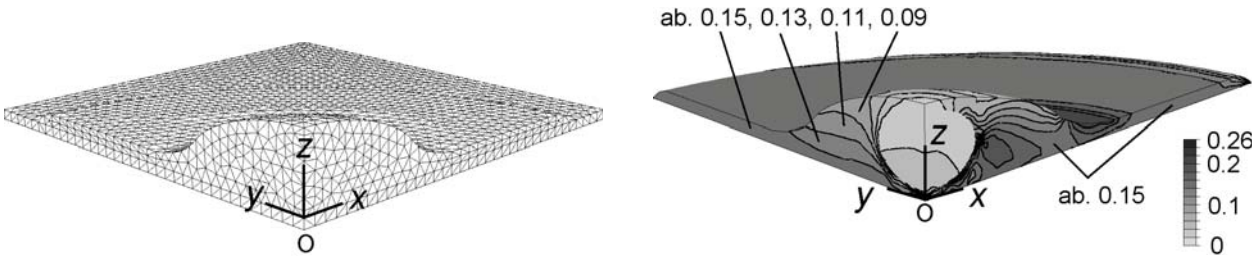

(a) (b)

Figure 8: (a) Finite element model of a quarter of an axisymmetric cell that adheres to the substrate and (b) distribution of the strain component in the stretching direction (x-axis) as a result of the finite element analysis with conditions of 15% tensile strain in the stretching direction and 4% compressive strain in the transverse direction (y-axis).

SFs in the strain-free angle also held for the cell axis (Wang *et al*., 2001).

According to Table 3, the mean angles of the basal SFs in isolated cells, *i.e.*, 74.2^o and 86.8^o, were 4-17^o different from the mean angles in the subconfluent cells, *i.e.*, 0.5^o and 70.2^o. The SD of the angle distribution, *i.e.*, 5.3^o, for the basal SFs in isolated cells with no apical SFs (n = 829) was 1.5 times larger than the angles in the basal SFs in subconfluent cells with no apical SFs (n = 1088), *i.e.*, 10.0^o, while the SD was almost equal to 10^o for isolated and subconfluent cells with apical SFs. The wider range of SF orientations in isolated cells with no apical SFs reflects that the SFs were distributed more irregularly. The cell-to-cell contact may influence the SFs to orient in the same direction.

To the best of our knowledge, no quantitative measurements of the orientation of apical SFs has been reported previously. Changes in SF angles occur in a matter of minutes, followed by changes in cell angles in a matter of hours (Takemasa *et al*., 1998; Wille *et al*., 2004). The distribution range of apical SFs is much narrower than that of basal SFs, as shown in Fig. 4. In the apical region, SFs will be subjected to a smaller strain, which might be $\sim$10% strain under a 15% strain acting on the substrate (see Fig. 8(b)). If a 10% cyclic strain is applied to the basal SFs, the strain limit hypothesis with a 5% strain limit (Yamada *et al*., 2002) predicts an angle range of $\sim$50^o (see Fig. 7).

Two types of hypotheses have been proposed to explain the orientation angle of SFs under cyclic stretching: one is that the SFs orient as to be subjected to a minimum strain (Wang *et al*., 1995; Takemasa *et al*., 1997, 1998) and the other is that SFs can orient if they are subjected to a strain that is less than a strain limit (Yamada *et al*., 2002). The former hypotheses recognize the reorientation of SFs as an optimum behavior while the latter recognize it as a survival technique. In spite of these different viewpoints, both hypotheses predict the same optimal angle. The strain limit hypothesis (Yamada *et al*., 2002) explains the most frequent orientation angle and permissible orientation range of SFs quantitatively. Nevertheless, this hypothesis does not describe an intracellular structure with parallel SF bundles. The dynamics of AFs should be incorporated to formulate SFs with such a structure (Civelekoglu *et al*., 1998; Yamada *et al*., 2006).

According to Fig. 7, more SFs are subjected to compressive strain than are subjected to tensile strain in the fiber direction under cycles of stretching and relaxation. (A process of SF deformation in the fiber direction is demonstrated for one cycle in Fig. 1 in Yamada *et al*., 2000.) A theoretical simulation shows that the orientation angles are between 51 and 64^o for SFs subjected to tensile strains (0 to 4%) and between 64 and 90^o for those subjected to compressive strains (0 to –4%). One of the reasons for this biased distribution might be that the range of angles (26^o) that corresponds to the range of compressive strains (0 to –4%) is two times greater than the range of angles (13^o)

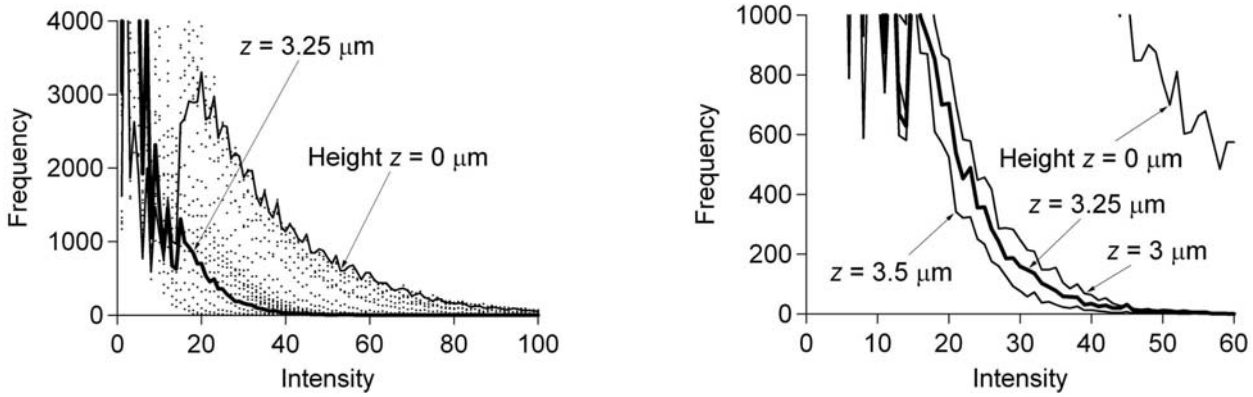

Figure 9: Intensity distributions (range 1-255) of the slice images of an isolated cell in Fig. 2. Intensity 0 of the background is neglected. Lines denote the intensity distributions on the height levels z = 0, 3, 3.25, 3.5 μm and dots denote the other height levels. Most of the apical SFs/AFs in the right panel of Fig. 2 have intensities ranging from 20 to 40.

corresponding to the tensile strains (0 to 4%).

Yoshigi *et al*. (2003) reported that the SD of the orientation distribution of SFs in confluent cells decreased progressively with durations of 0.5, 1, 2, 5, 10, and 20 h without changing the mean angle under almost pure uniaxial stretching with a 10% strain range. The SD of the SF angles in their study was 39^{o} after 2 h and 14^{o} after 20 h. The conditions in our study were 2 h of stretching with a 15% strain range. According to Figs. 5 and 6, the SD of the basal SF angles in our study was roughly 10^{o} after 2 h, which is close to the SD value after 10 h rather than the value after 2 h with a 10% strain range. Takemasa *et al*. (1997) showed that a larger strain range accelerates the completion of SF orientation. Therefore, in our experiments, the subconfluent cells might have almost completed the reorientation of basal SFs, and the isolated cells might have been approaching completion.

Figure 9 shows the intensity distributions (range 1–255) for various heights of slice images (330 $\times$ 510 pixels) of the isolated cell shown in Fig. 2. Intensity 0 of the background was neglected. In the figure, lines denote the intensity distributions on the height levels z = 0, 3, 3.25, and 3.5 μm, and dots indicate the other height levels. The slice image with the largest intensity was determined to be the cell bottom, which had a height of z = 0. The angle of the basal SFs was measured for that image. Most of the apical SFs/AFs in the right panel of Fig. 2 had intensities ranging from 20 to 40. The basal membrane cannot be identified accurately from a series of fluorescent images because they only provide the intensity distributions of SFs/AFs. The sliced image chosen to measure the angle of apical SFs/AFs does not have the peak intensity among those above and below the selected image. This might have occurred because the total intensity in the pixels decreases with the height level due to the reduction of the cell volume for the confocal laser scanning microscopy measurements.

To estimate the error of the SF angles, we first checked the variation of the SF angle due to the nonuniform deformation of substrate by numerically estimating the values using Eqs. (2) and (3). Using the strain variations resulting from the nonuniform deformation of the silicone membranes, mean $\pm$ 2 SD, *i.e.*, (λ_x-1, λ_y-1) = (0.151,-0.044), (0.158, -0.044), (0.151,-0.040), and (0.158,-0.040), the orientation angles were estimated to be 62.7^{o} (minimum), 63.2^{o}, 63.9^{o}, and 64.5^{o} (maximum), respectively. The difference between the maximum and minimum angles was at most 2.0^{o}, indicating that the effect of nonuniform deformation in the region of interest was very small compared to the distribution range of SF angles. Second, we estimated the angle error as $\tan^{-1}(1/56)$ = 1.0 ^{o} for an extreme case in

which one corner of a rectangular silicone chamber (56 mm $\times$ 35 mm) was misplaced on a microscope stage with a 1-mm offset in the transverse direction.

In the future, we will study dose-dependent responses, *i.e.*, stretching magnitude and stretching duration, to ascertain the quantitative effect of the mechanical stimulus on SF/cell orientation responses.

Acknowledgement: This work was supported by a Grant-in-Aid for Scientific Research on Priority Areas (No. 15086213) from the Ministry of Education, Culture, Sports, Science and Technology of Japan.

References

1. **Civelekoglu, G., Tardy, Y., Meister J.-J.** (1998): Modeling actin filament reorganization in endothelial cells subjected to cyclic stretch. *Bulletin of Mathematical Biology*, vol. 60, pp. 1017–1037.

2. **Dartsch, P. C., Betz, E.** (1989): Response of cultured endothelial cells to mechanical stimulation. *Basic Research in Cardiology*, vol. 84, pp. 268–281.

3. **Dejana, E., Corada, M., Lampugnani, M. G.** (1995): Endothelial cell-to-cell junctions. *FASEB Journal*, vol. 9, pp. 910–918.

4. **Flaherty, J. T., Pierce, J. E., Ferrans, V. J., Patel, D. J., Tucker, W. K., Fry, D. L.** (1972): Endothelial nuclear patterns in the canine arterial tree with particular reference to hemodynamic events. *Circulation Research*, vol. 30, pp. 23–33.

5. **Iba, T., Sumpio, B.** (1991): Morphological response of human endothelial cells subjected to cyclic strain in vitro. *Microvascular Research*, vol. 42, pp. 245–254.

6. **Ingber, D. E.** (1997): Tensegrity: the architectural basis of cellular mechanotransduction. *Annual Review of Physiology*, vol. 59, pp. 575–599.

7. **Kano, K. Katoh, K., Fujiwara, K.** (2000): Lateral zone of cell–cell adhesion as the major fluid shear stress-related signal transduction site. *Circulation Research*, vol. 86, pp. 425–433.

8. **Kataoka, N., Ujita, S., Kimura, K., Sato, M.** (1998): The morphological responses of cultured bovine aortic endothelial cells to fluid-imposed shear stress under sparse and colony conditions. *JSME International Journal*, Series C, vol. 41, pp. 76–82.

9. **Lampugnani, M. G., Corada, M., Caveda, L., Breviario, F., Ayalon, O., Geiger, B., Dejana, E.** (1995): The molecular organization of endothelial cell to cell junctions: differential association of plakoglobin, β-catenin, and α-catenin with vascular endothelial cadherin (VE-cadherin). *Journal of Cell Biology*, vol. 129, pp. 203–217.

10. **Langille, B. L., Adamson, S. L.** (1981): Relationship between blood flow direction and endothelial cell orientation at arterial branch sites in rabbits and mice. *Circulation Research*, vol. 48, pp. 481–488.

11. **Sipkema, P., van der Linden, P. J. W., Westerhof, N., Yin, F. C.-P.** (2003): Effect of cyclic axial stretch of rat arteries on endothelial cytoskeletal morphology and vascular reactivity. *Journal of Biomechanics*, vol. 36, pp. 653–659.

12. **Stamenovic, D., Ingber, D. E.** (2002): Models of cytoskeletal mechanics of adherent cells. *Biomechanics and Modeling in Mechanobiology*, vol. 1, pp. 95–108.

13. **Takemasa, T., Sugimoto, K., Yamashita, K.** (1997): Amplitude-dependent stress fiber reorientation in early response to cyclic strain. *Experimental Cell Research*, vol. 230, pp. 407–410.

14. **Takemasa, T., Yamaguchi, T., Yamamoto, Y., Sugimoto, K., Yamashita, K.** (1998): Oblique alignment of stress fibers in cells reduces the mechanical stress in cyclically de-

forming fields. *European Journal of Cell Biology*, vol. 77, pp. 91–99.

15. **Wang, H., Ip, W., Boissy, R., Grood, E. S.** (1995): Cell orientation response to cyclically deformed substrates: experimental validation of a cell model. *Journal of Biomechanics,* vol. 28, pp. 1543–1552.

16. **Wang, J. H.-C., Goldschmidt-Clermont, P., Moldovan, N., Yin, F. C.-P.**, (2000a): Leukotrienes and tyrosine phosphorylation mediate stretching-induced actin cytoskeletal remodeling in endothelial cells. *Cell Motility and the Cytoskeleton*, vol. 46, pp. 137–145.

17. **Wang, J. H.-C., Goldschmidt-Clermont, P., Yin, F. C.-P.** (2000b): Contractility affects stress fiber remodeling and reorientation of endothelial cells subjected to cyclic mechanical stretching. *Annals of Biomedical Engineering*, vol. 28, pp. 1165–1171.

18. **Wang, J. H.-C., Goldschmidt-Clermont, P., Wille, J., Yin, F. C.-P.** (2001): Specificity of endothelial cell reorientation in response to cyclic mechanical stretching. *Journal of Biomechanics*, vol. 34, 1563–1572.

19. **White, G. E., Fujiwara, K.** (1986): Expression and intracellular distribution of stress fiber in aortic endothelium. *Journal of Cell Biology*, vol. 103, pp. 63–70.

20. **Wille, J. J., Ambrosi, C. M., Yin, F. C-P.** (2004): Comparison of the effects of cyclic stretching and compression on endothelial cell morphological responses. *Journal of Biomechanical Engineering*, vol. 126, pp. 545–551.

21. **Yamada, H., Matsumura, J.** (2004): Finite element analysis of the mechanical behavior of a vascular endothelial cell in culture under substrate stretch. *Transactions of the JSME*, Series A, vol. 70, pp. 710–716 (in Japanese).

22. **Yamada, H., Mouri, N.** (2006): Measurement of the contours of cultured vascular endothelial cells on a stretched substrate with confocal laser scanning microscopy. *Proceedings of the Mechanical Engineering Congress, 2006 Japan*, vol. 5, pp. 221–222, JSME (in Japanese).

23. **Yamada, H., Takemasa, T., Yamaguchi, T.** (2000): Theoretical study of intracellular stress fiber orientation under cyclic deformation. *Journal of Biomechanics*, vol. 33, pp. 1501–1505.

24. **Yamada, H., Morita, D., Matsumura, J., Takemasa, T., Yamaguchi, T.** (2002): Numerical simulation of stress fiber orientation in cultured endothelial cells under biaxial cyclic deformation using the strain limit hypothesis. *JSME International Journal*, Series C, vol. 45, pp. 880–888.

25. **Yamada, H., Ando, H., Morita, D.** (2006): Numerical simulation of the effects of actin binding and cellular deformation on the orientation of actin stress fibers under cyclic stretch. In: Wada, H. (ed.), *Biomechanics at Micro- and Nanoscale Levels*, Vol. II. Hackensack, NJ: World Scientific, pp. 149–159.

26. **Yoshigi, M., Clark, E. B., Yost, H. J.** (2003): Quantification of stretch-induced cytoskeletal remodeling in vascular endothelial cells by image processing. *Cytometry*, Part A, vol. 55A, pp. 109–118.